FRACTURE ANALYSIS IN METALLIC MATERIALS

Isaias Gallana, Fernando Cordisco

CE597 Final Project

ABSTRACT

The fracture behavior in metallic structures is studied in this work. The material selected to perform the studies is Al 2024 (copper + magnesium, aluminum alloy) which is widely used in aeronautics structures. Mode-I and Mixed-mode test were performed. For the mixed mode tests a Arcan device was constructed and the details of the construction are presented herein. Analytical and numerical studies were correlated with the experimental results in mode-I to investigate which would be the best fracture material parameter to be used in metals. We have studied the K-field, J-Integral, CTOD and cohesive criteria and we found, in our opinion, that the best choice in order to compare the fracture resistance in this kind of materials would be the CTOD method. The constitutive parameters extracted with the cohesive zone models still could be an acceptable choice but for really specified conditions. The mixed mode tests showed good results nevertheless the results from the test were lost and no data could be compared.

INDEX

1.- OBJECTIVES

The main objective of this study is to characterize the fracture behavior in metallic materials and discuss the different model and methodologies to extract fracture data parameters. To perform the complete set of experiments, as an extra objective a mixed-mode Arcan fixture was developed.

2.- INTRODUCTION

The metallic copper-magnesium aluminum alloy (Al 2024) is a widely used material in the aeronautic industry. Since 1931 replaced the duraluminum material because of its large strength-to-weight ratio and excellent fatigue resistance. Nowadays is specially used as wing and fuselage folding. Even is one of the most strength aluminum alloys, is one of the less ductile in its family and therefore it's an interesting material to study under crack propagation.

Fig. 2.a. - SONAER acrobatic airplane. All the wings skin is made in aluminum 20204 T3

Because of the different airplane parts in which this isotropic alloy can be used this project is focused to study the fracture process in an opening mode (mode-I) but also allow the characterization for different in plane load combinations (mixed mode).

For the mode-I tests, edge notch samples (Fig 2.b) were developed to run experiments and compare the typical methods to characterize fracture parameters. Specifically, the K-field, J-integral, CTOD and Cohesive models were studied. In this regard the works of [dodds], [Sutton], [alfano], [zavattieri] where used as guideline for the study.

For the mixed mode tests it was necessary to design and develop a special fixture to allow the tensile machine to apply load at different angles. The fixture constructed (Fig. 2c) was the Arcan [*] or Brazilian nut device [references] and it correspondent special samples. With this fixture two tests were performed: (1) first test at 0° to compare results with the edge notch test, (2) test the capabilities of the fixture at different angles and if possible measure the critical load to propagate the crack.

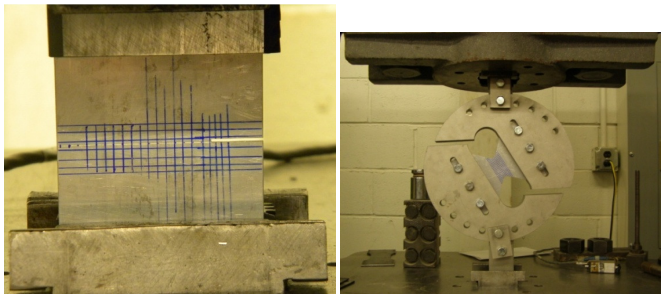

Fig. 2 – (b) left picture Edge notch sample, (c) right picture arcan fixture with special mixed mode sample

3.- TEST EQUIPMENT

To design the samples and the arcan fixture the limiting constraint was defined by the tensile machine which is placed in the Material Concrete Lab of the Civil Department of Purdue University and is designed to carry extremely large load compared to the typical resistance of a aluminum sample and with a load cell sensivity of 500kg. In this sense both: (i) the size of the aluminum specimens and (ii) the size of the arcan fixture were designed to obtain appreciable values.

3.1- Design of the Arcan Device.

After doing a quick search in the available literature we could came out with a design that fits our needs. We can mention some of the author as Sutton, Deng, Dodd in which we base our design. See reference[1].

3.1.1- Characteristics of the parts.

- Thickness= 1/2 in
- Material A304.
- The device allows mix mode with 7 different angles, from 0 to 90 degrees with a variation of 15 degrees between each point.

3.1.2 - Dimensions

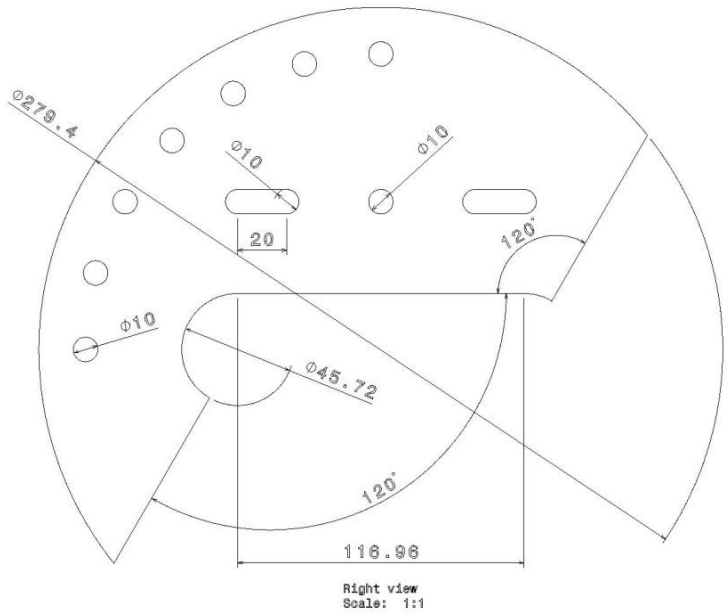

Figure 3.a. Dimensions [mm]

- [1] Sutton, Deng: Development and application of a crack tip opening displacement-based mixed mode fracture criterion

- Roychowdhury, Das Arun Roy, Dodds. Ductile tearing in thin aluminum panels: experiments and analyses using large-displacement, 3-D surface cohesive elements

3.2 - Assembly.

Four (4) parts form the whole device. Two of these semicircle parts form a circular plate.

The sample to be test is hold between those circular plate using hard steel bolds of 1 cm diameter in 6 point. Four of these holds allow same variation in the horizontal direction as it can be seen in the figure 3.a. The following picture shows the device completely.

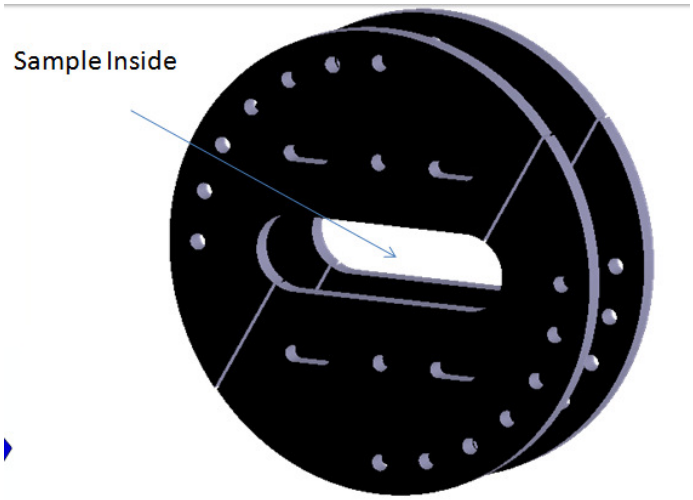

Figure 3.b. – Disposition of the parts.

3.2.1 - Mechanical interface with the Tensile Machine.

As the machine do not present a properly clamp to hold this device, we built an adaptation for this purpose. It was made using the remaining material of the construction of the pieces showed before.

The following pictures show the mechanical interface.

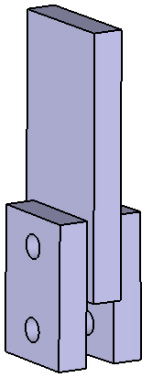

Figure 3.c. – Mechanical interface.

In the next the dimensions are presented

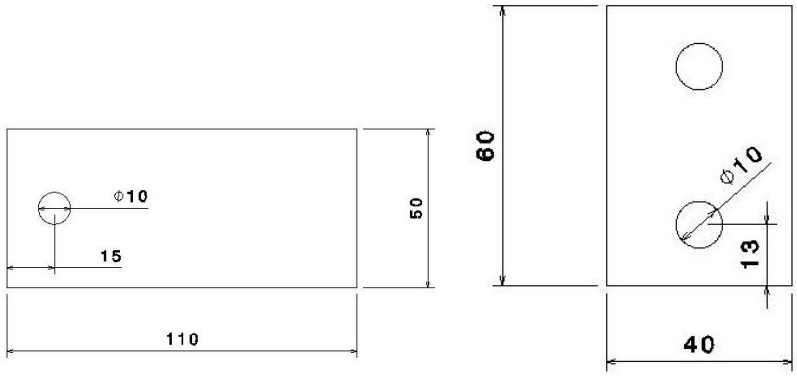

Figure 3.(e), (d) – Interface component [mm].

So, we can see all the part together. These parts are hold to the circular plates of the Arcan using hard steel bolds 1 cm diameter and them mounted to the tensile machine.

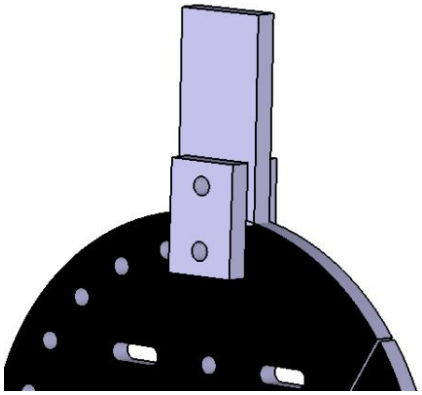

Figure 3.f. – Assembly of the interface in the device.

3.3 - Numerical simulation results.

In order to have a value of the deformation of the system we did some numerical analysis of the parts. For that purpose we modeled one of the parts using shell element. We constrain the moment in the vertical direction and we applied a stress in the corresponding hole. The strain applied to the hole corresponds to two (2) times the Yield Stress of a Aluminium 2024 T3. So at the end we have a device design with a security factor of four (4). In the next, the results for the displacement field are presented (results are en meters).

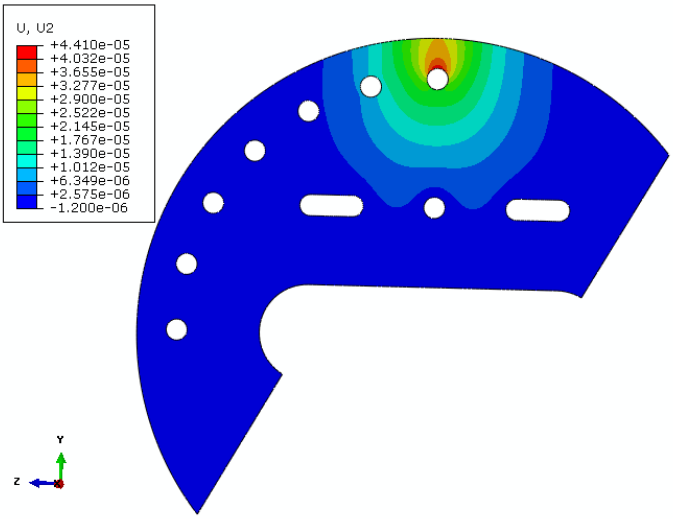

Figure 3.f. – Displacement field of the component [meters].

Also we simulate the mechanical interface between the Arcan device and the Tensile Machine. We only simulate the critical component of the group. The load applied to this part was four (4) times the yield stress of Al 2024 T3. (Results are in meters and Pa)

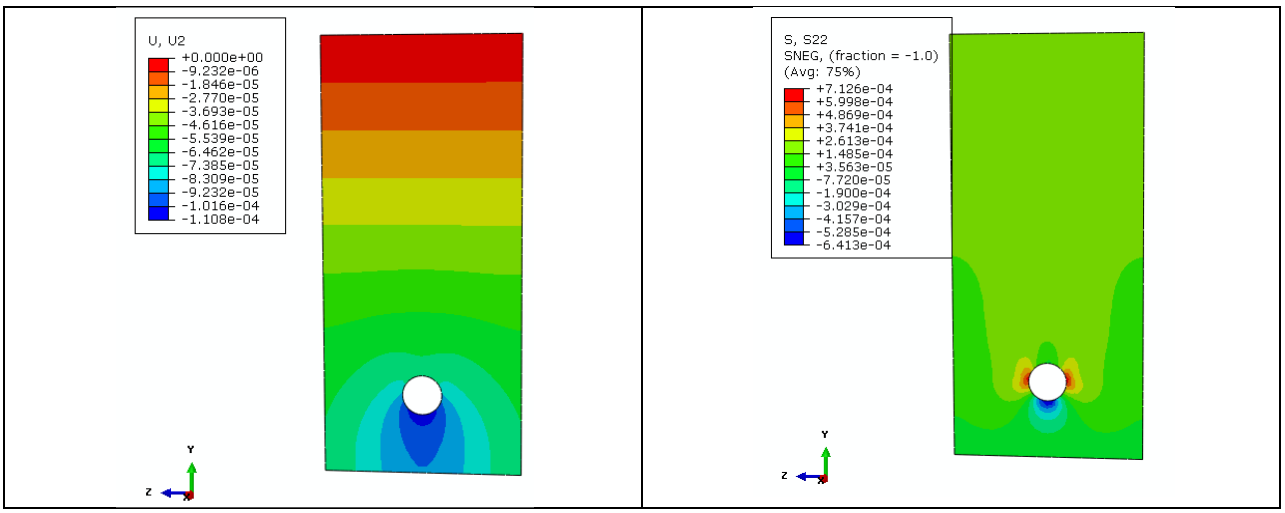

Figure 3.g. – Stress and displacement field of the interface component.

The total displacement in the device is too small compare with the displacement of the sample.

3.4 - Fabrication.

All the pieces were made from one sheet of 24 x 12 x ½ inches of A304.

We use as a cutting tool, a water-jet machine. So, all the parts were design using a Cad Software compatible with the software of this machine. For that reason all the part were presented in *.dxf files. Previously to cut the samples, a simulation of the whole cut was done, using the software provided by this machine.

Here we show some picture with the arrange of the pieces in the rectangle plate before cutting it. An image of the flow pad is presented too.

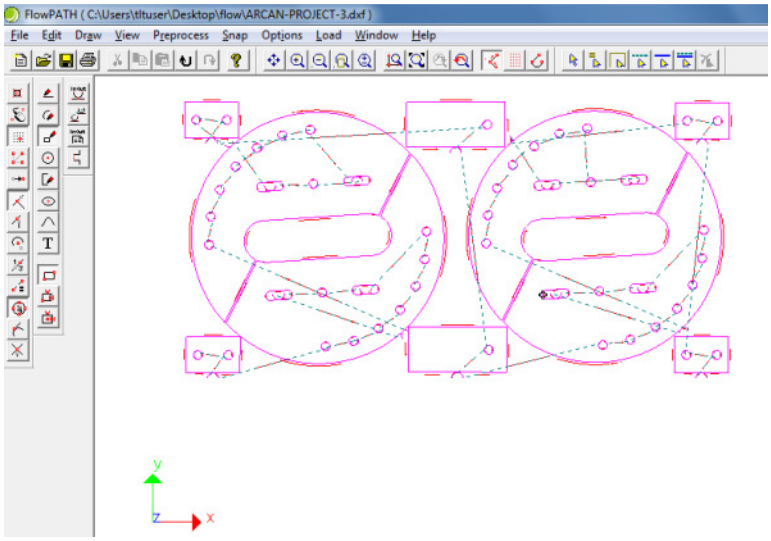

Figure 3.h. – Disposition of the pices in the steel plate before cutting. Flow path of the water jet machine.

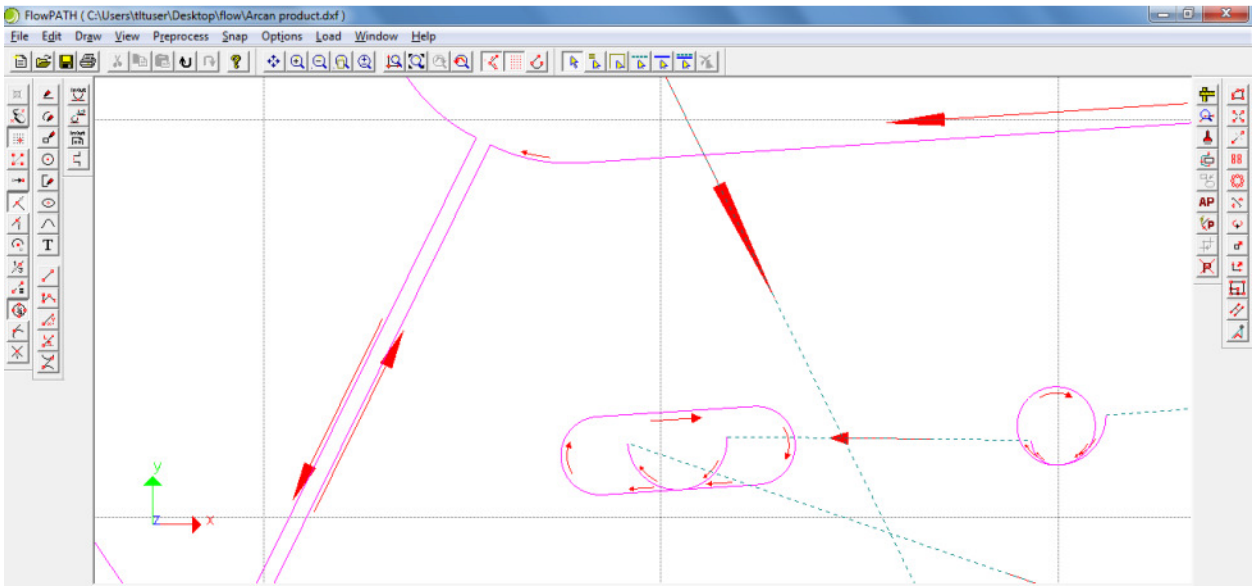

Figure 3.i. – Flow path of the water jet machine.

The red arrows with pink solid lines show the path of the machine during the cutting, while the red arrows with dashed blue lines show the path of the head of the machine from one point to another between cuts.

3.5. - Design and fabrication of the specimen.

We made two types of specimen: one type correspond to the one used for the Arcan device and the other is a tipical Edge Notch Sample.

The dimension was suggested in order to be inside the range where the Tensile machine could measure due to its load cell. In the next the dimensions for each sample is presented:

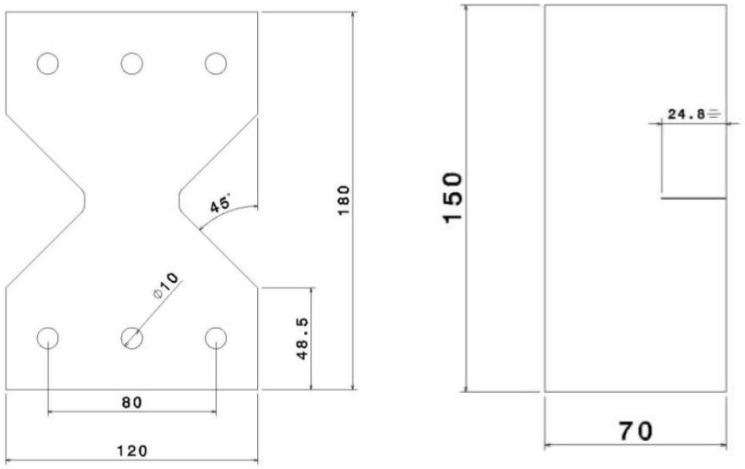

Figure 3.j. – (left): Arcan sample. (right) Edge notch sample. All the dimensions in dimension [mm] [2]. The thicknesses of those specimens were 2 mm.

As explained in the introduction, the samples were made of Al 2024 T3 with a Elastic modulus of E=71 GPa and a Yield strength of σy= 290 Mpa. In the next the used Stress-Strain plot is presented.

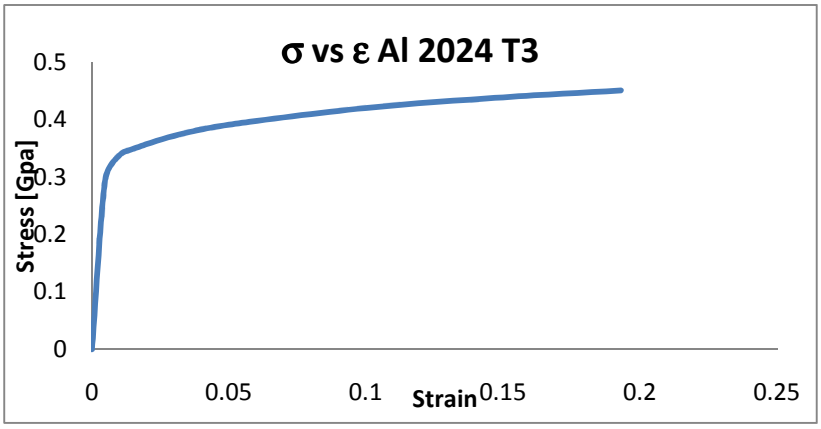

Figure 3.l. - σ vs ε of aluminum 2024 T3

[2] For the purpose of our test we did a notch of 6 mm in these samples.

3.5 - Test implementation.

We use an LVDT for measuring displacement…..

3.6 – Local displacement parameter extraction (DIC)

In order to extract local values of relative displacement around the crack to be used later for the material characterization a fine mesh of 3mm was drawn around the expected region of crack propagation. The size of the grid was defined to be on the order of the plastic region developed around a crack. To calculate the plastic radius a estimation by the use of equation 3.1 [Anderson] augmented by the Irwin factor for metallic materials [Anderson], equation 3.2.

$$rp^* = \frac{KIC^2}{2\pi\sigma_{ys}^2} \quad (3.1)$$

$$r_p = 2.rp^* \quad (3.2)$$

The yield strength for the Al2024 T3 is 290Mpa while a estimated KIC provided for the 2024 is around 25Mpa.a1/2 and 30Mpa.a1/2. By the use of this last value the estimated plastic radius is of 3.5mm, so the grid was done of 3mm as shown in Fig. 3.1. During the test a set with a camera and a clock where used to relate the displacement with the load applied (Fig. 3.1.)

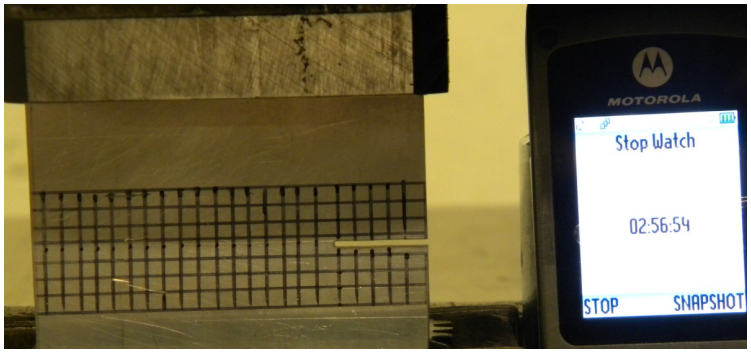

Fig.3.1.– Mesh Grid to extract displacement data. A fixed camera took photos and at the same time the time for each photo was recorded by the watch. Later by measuring the pixels we were able to calculate the relative displacement and correlate it with the P-d curve. Grid size= 3mm

4. – EXPERIMENTAL RESULTS

4.1 – Edge notch sample n1- Mode I

The purpose of this test is to obtain the parameter needed for generated a cohesive low and the information for construct the curves that related the crack tip opening displacement (CTOD).

Particularly in this test we had some slipper between the clamps and the sample. So we can see in the final picture the relative angle between the parts. We think that this is the reason of the not common crack pattern in the sample.

Unfortunately we could not get the data from this test. So we were unable to post process the information obtained here. In the next the crack growth sequence is presented

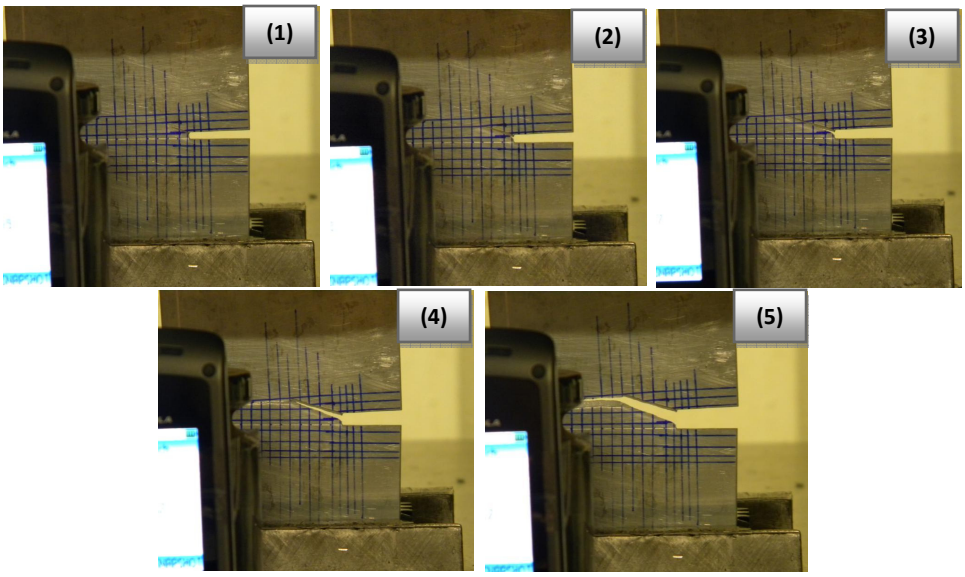

Figure 4.a

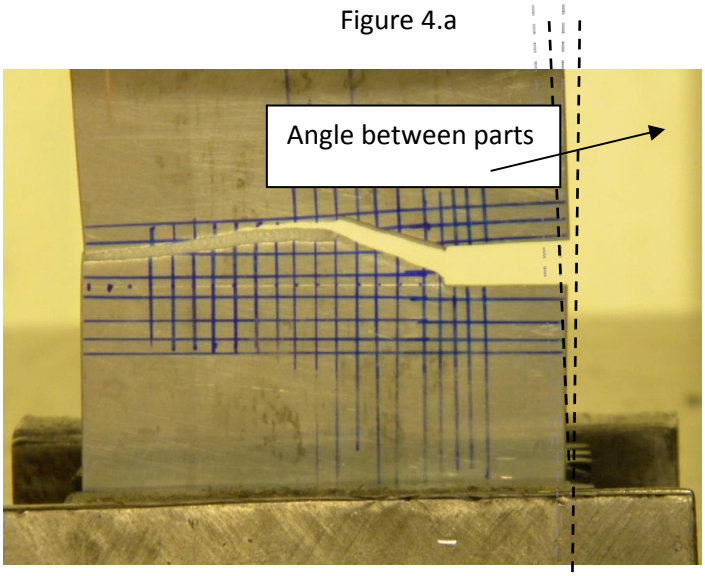

Figure 4.b – Crack pattern. Angle between parts after the catastrophic propagation of the fracture.

4.2 – Edge notch sample n2 - Mode I

The purpose of this test was to obtain the same parameters describe in before. We had planned it in order to have redundant data of the test. But due to the failure in obtain this information this was the only test in which we could get the information required. I the next is the load displacement curve obtained from the Tensile machine.

We can see in the Load – displacement curve (figure 4f) a slow response of the sample due to the increment in displacement. This behavior is explained because of the slipper between the clamps and the sample. We were located the LVDT not in a position where only could measure the displacement of the sample, so in this case it is measured the displacement of the moving parts of the machine that holds the clamps. We could see also the pick load for this test 3100 Kgf in the order of magnitude we expected.

We are presented here also a sequence of picture showing the crack grow in the sample.

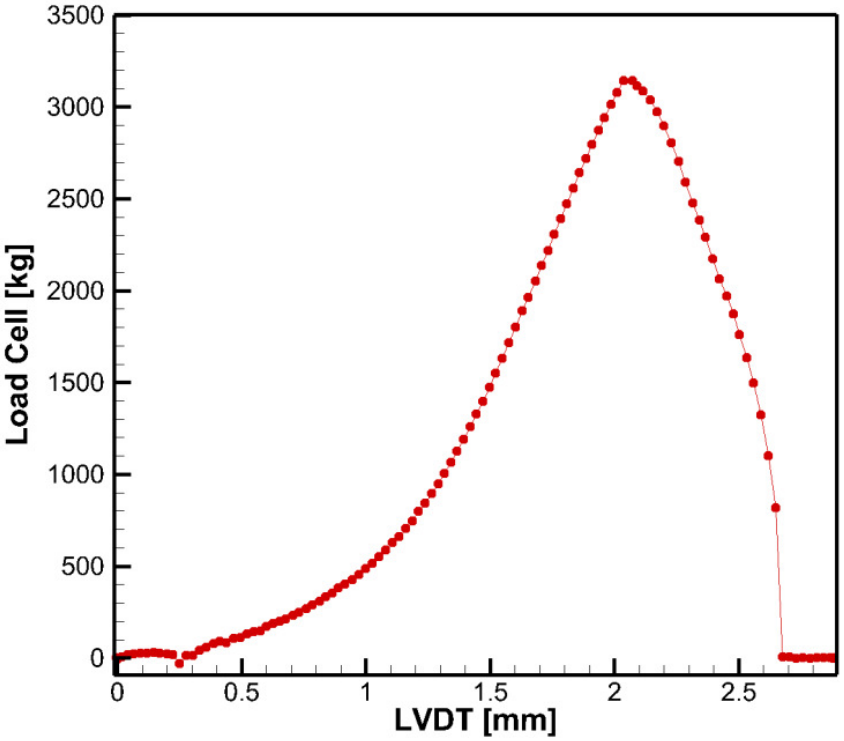

Figure 4.f – Load vs displacement curve.

Sequence:

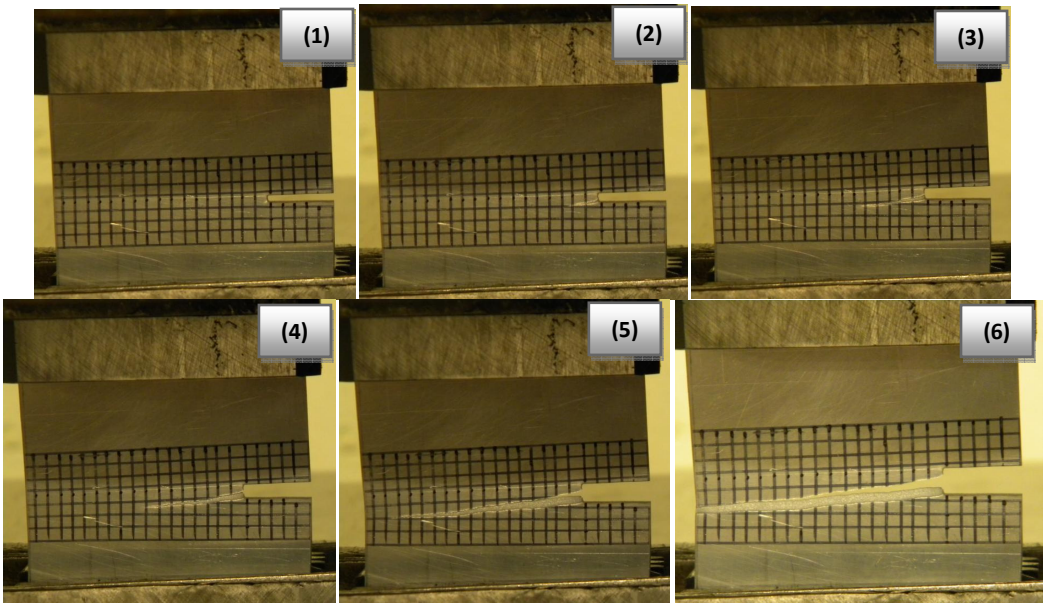

Figure 4.g

4.3 - Arcan Sample- Mode I

The purpose of this test was to validate the design of the arcan device. For that reason we performed a mode I test. We expected to compared the result obtained in this test which the one obtained using the edge notch sample. Due to the fact that we could not obtain the data for this test we couldn't correlated the result. Even thought we could see a similar crack pattern to the mode I test that we had done with the edge notch sample. So we could conclude here that the device works properly, as it was design. During the test and before it we did a close look to the device in order to see possible deformation of the component or any other problem. We do not detect anything critical here.

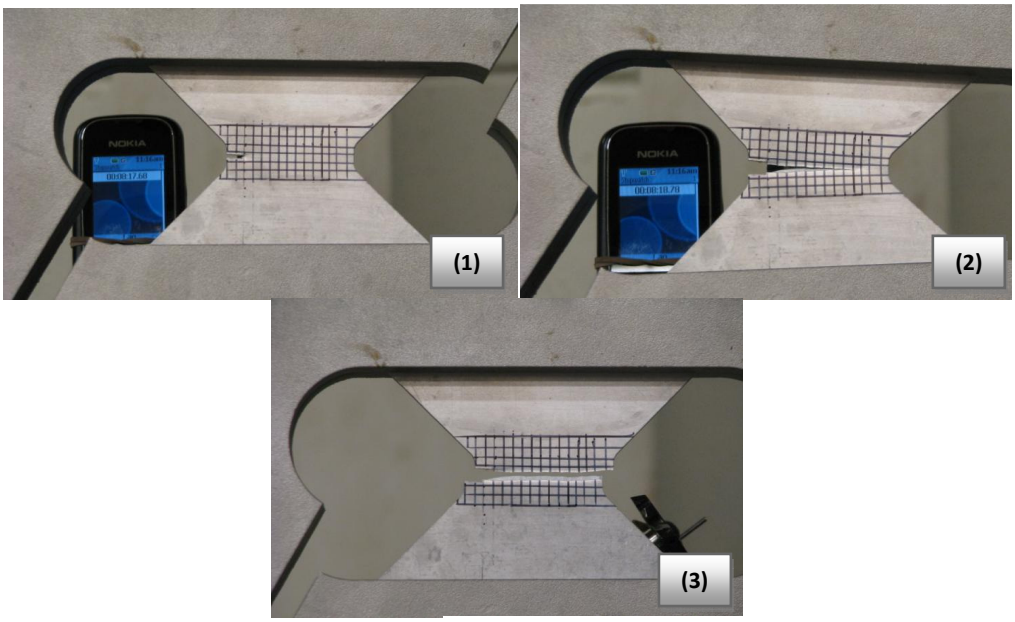

Fig. 4h

4.4 - Arcan sample - Mix Mode [60 degrees]

The purpose of this test was to obtain data from a mix mode test and to see how the arcan device works in a mix mode condition. From the implementation point of view, the device was easy to implement and attach to the machine in a mix mode condition. In fact we can say that this operation did not change from a pure mode condition.

We are not familiar with mix mode test and even more, in this test we could not get the data from the experiment, so we just have seen the behavior of the crack as a spectator.

Here are some sequence of picture that shows the behavior of the crack.

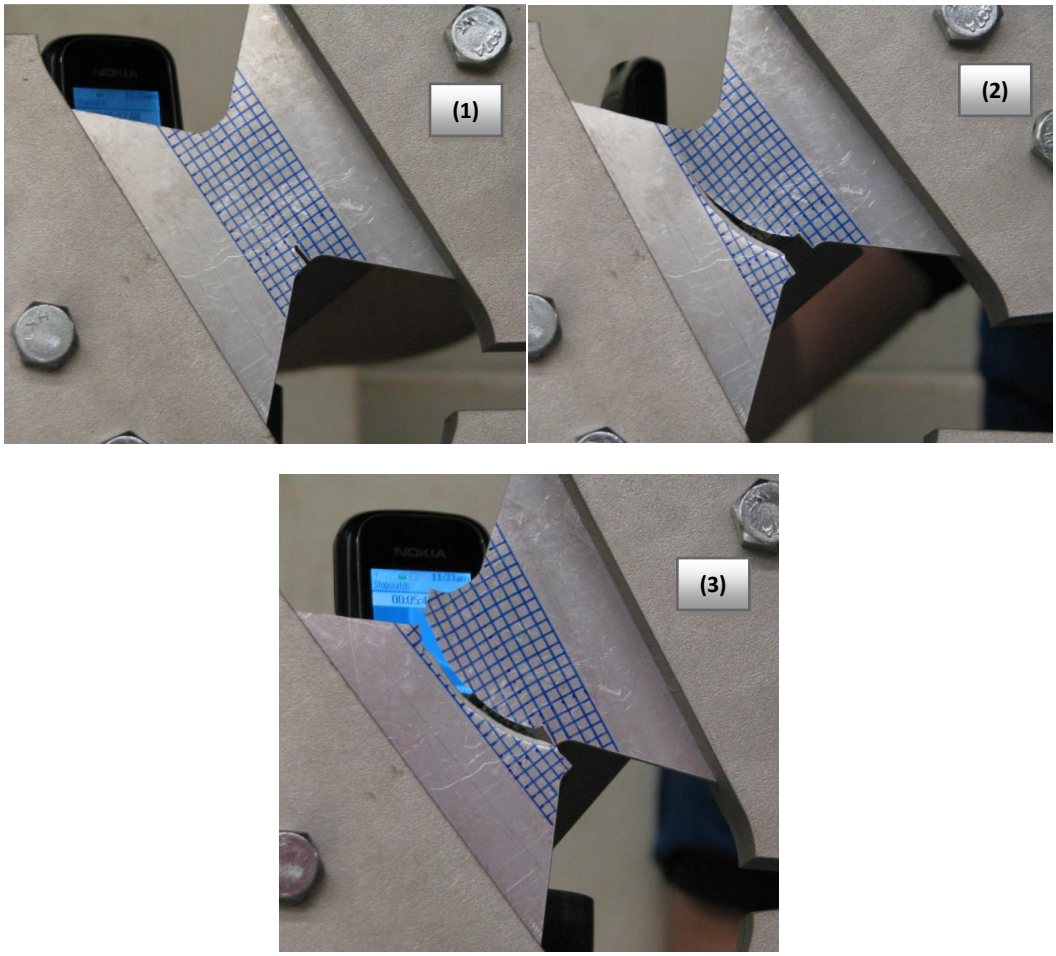

Figure 4.i.

4.5 – Characteristic of the crack in the thickness.

One of the things to emphasize here is the crack shape in the sample.

We could see in every sample, after its fails, a triangular cut. (see picture below)

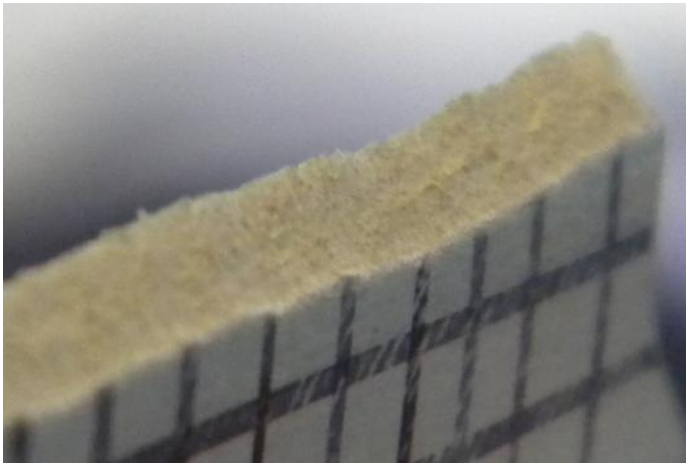

***Figure 4.s. Characteristics of the crack in the thickness. Shear fracture*.**

We can explain this phenomenon due to the stresses in the crack tip.

We can see in the following picture a combination of plane stress and plane stress in the crack tip as we increase the size of the thickness in a plate. [Anderson chapter 5]

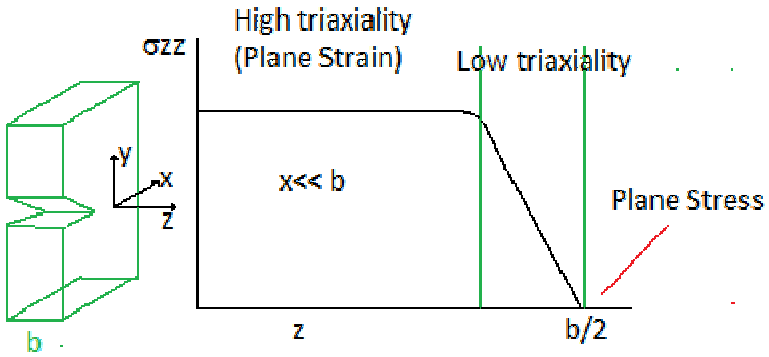

Figure 4.t. Schematic variation of transversal stress and strain through the thickness at a point near the crack tip.

The presence of triaxial stresses in the thickness of a material generates void nucleation grow of voids and coalescence of voids (tunneling), generating a flat crack in the center (plane strain) with bands at 45 degrees in the sides (plane stress).

Here we show some pictures of the phenomenon.

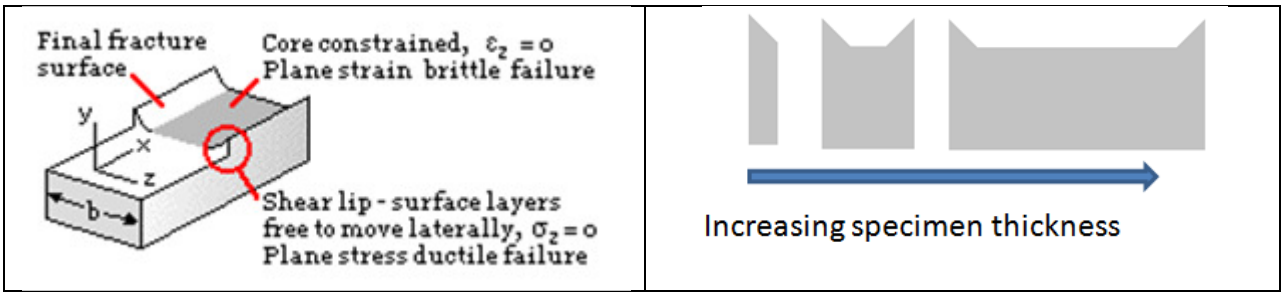

Figure 4.u. Effect of specimen thickness on fracture surface morphology for materials that exhibits ductile crack growth.

5. - MODE-I FRACTURE PARAMETERS EXTRACTION

Unfortunately the Load-Displacement data recorded for the mixed mode testing was lost and no conclusions can be discussed in this regard. Nevertheless the mode-I results from the arcan test have shown the same crack pattern as the mode-I edge notch test, which means that the arcan test is effectively applying a mode-I condition. But still no conclusion on the change between the critical load from mode-I to mixed mode conditions can be discussed. Nevertheless we can still study the different methodologies for crack propagation by the use of Mode-I experiment.

In addition is important to remark that as explained in the introduction the main objective of this section is to not to do exact models and calculations on the studied parameters but to (i) study the model methodologies to extract material data, and (ii) discuss the applicability and limitation of this models for the engineering practice in order to define which method would be the most cost-effective solution to extract this material data.

5.1.- K-field Fracture method

The simplest approach to characterize fracture resistance of a material would be by the concept of fracture toughness KIC. However this approximation would lead to errors because in metals we have large damage spread by plasticity and stable crack growth after the load peak that causes crack growth. This last two considerations contradict the fundamental definition of the K-field which is developed with elasticity theories, and that can only be extended in specific situations to small scale yielding.

Nevertheless we can still find that providers of aluminium that still provide the KIC value. In this section we present the result of KIC for our test but we remark that this constant is mostly related to a load-critical parameter which will be highly dependent on the kind of test and dimensions of the sample and could only be used as a pseudo-characteristic parameter of the material and only for qualitative purposes. Thus, if we measure the critical load from the P-d curve (FIG4f) we can estimate a rough parameter by the use of equation (5.1.1).

$$K_{Ic} = Y \cdot \sigma_c \sqrt{\pi a} \quad (5.1.1)$$

Where Y is a geometric parameter that we took as one. σ_c is the remote stress obtained for the dimensions of the edge notch sample and using the peak load of 3142kg. Thus we obtain KIC=29.3 Mpa.$m^{1/2}$. As noticed, this value is close to the published values for the KIC which is around 25 Mpa.$m^{1/2}$ to 30Mpa.$m^{1/2}$.

5.2.- J-integral method

The J-integral is another approach that could be used to study the energy needed to propagate a crack. It has to be noticed that the J-integral is only valid when the integration is path independent [**rice**]. If we assume that plasticity can be studied as a monotonic non-linear elastic material, then the J-integral can be solved by means of a numerical method. To do so, we have used Abaqus with the "contout integral" option. The model was developed to meet the geometrical conditions of the edge notch sample and the remote displacement applied was set to the maximum displacement of the P-δ curve (Fig. 5.2.a) just at the instant before the crack started to propagate (i.e. the displacement associated to the peak load). We could also had selected the maximum displacement to account for the total energy up to the system was completely broken but to do so a great number of calculations with different crack length should be performed and is not the objective set in this analysis.

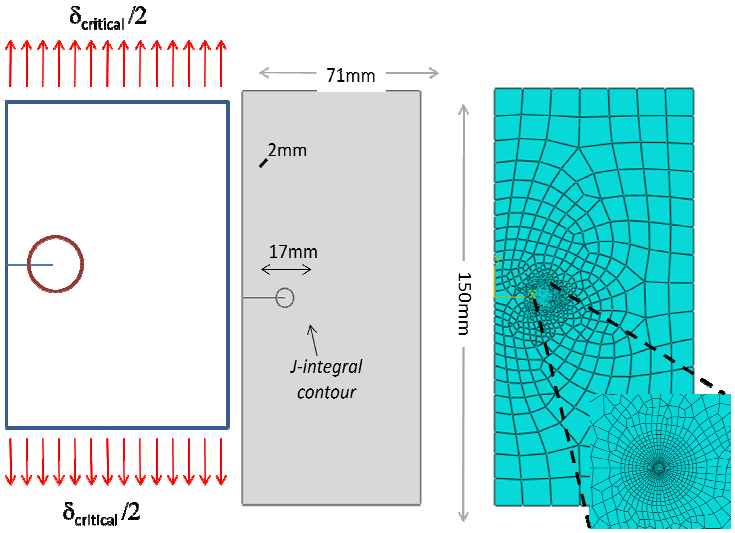

Fig. 5.2.a - (i) conceptual picture of the domain selected to calculate the energy release rate (δ_{max}=2.7mm). (ii) Abaqus geometrical model. (iii) Abaqus mesh + seem crack + contour integral calculation. We assume the crack growth in the direction of the crack

If we run the simulation we obtain the results presented in Fig. 5.2.b. The first thing to be noticed is that for the applied remote displacement condition, the value of strain obtained around the crack tip is extremely large (around 270%) which means that the problem cannot be studied by a small scale yielding theory. This means that the hypothesis to justify plasticity as a non-linear monotonic elastic curve is not valid anymore and that the J-integral is path dependent close to the crack tip. We could still make a rough approximation by evaluating different contours up to the point where we find the integral to be path-independent (this would be when we enclose the entire plastic region by the integral) and obtain an energy release rate for the material. Nevertheless this energy release rate will account not only for the energy required to open the crack but also for the energy dissipated by plasticity; which is not the energy that characterizes the fracture process as stated from the theory of fracture mechanics. However to have this rough value we did the calculation. We first found that the J-integral becomes path independent after a contour of an approximate radius of 3.5mm (which we notice is about the plastic radius value we have estimated with the analytical tools), and over that region the J-value converges to about J=261.5 kN.m

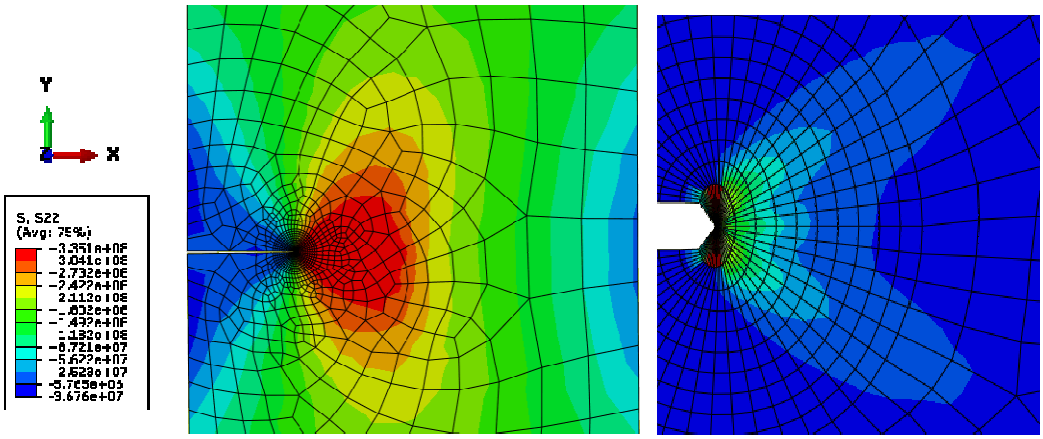

Fig. 5.2.b. (Left): S22 stress field. (Right): Plastic Strain field distribution

As a conclusion, even this value would be a better parameter than the KIC, it still lacks of a full theoretical grounding to support the parameter as a fracture material characteristic in the case of large yielding materials like the aluminum studied, and in our opinion this criterion would also not be a good choice to characterize fracture in metals.

5.3 – Cohesive Zone model

Another model that became more used in the last decade is the Cohesive Zone Model. The cohesive zone model states that the fracture process is not controlled only by a energy criterion but by a cohesive material parameter which is function of the local damage around the crack tip. This damage region where the damage nucleates and coalesce before the crack propagates is controlled by a constitutive law known as cohesive law. Thus the cohesive law is a characteristic of the material and controls the crack propagation in it. The law is characterized by the following parameters:

1) Shape (accounts for the total local energy and its distribution)
2) Maximum local strength/traction
3) Critical local displacement

Where the word “local” refers to the values of this parameters in the region where the damage is growing before the crack propagates. This region is defined as a material parameter and is known as cohesive length.

Based on this last explanation it can be noticed that this constitutive models are much more complex than the last two criteria. Now the crack in a material is not controlled just by one parameter but by three parameters: shape, maximum traction, and critical displacement. I theory this concepts are much more consistent as fracture parameters, but a complete extraction of this parameters by means of experimental results is not possible nowadays. In this section we discuss one of the typical procedures used to measure this parameters.

Nowadays there are developed a wide range of potential laws that account for the shape of a cohesive law. Nevertheless most of these shapes are defined a priori as a fixed parameter and usually based on qualitative and best fitting considerations. In our case, to simplify the calculations, we make the first “big” hypothesis and we decide to fix it as a triangular law. It should be noticed that for metals

is most common the use of T-H or X-N laws. Once the shape is defined there still three unknowns from the problem: the energy under the curve (critical cohesive energy), the maximum traction, and the critical displacement. All this parameters should be obtained from the experiment (Fig. 5.3.a). As we have three unknowns and only one experiment the only possible solution would be to develop a computational model (Fig.5.3.b) and preselect these values up to find that the computational load-displacement curve obtained as an outcome of the selected cohesive parameters matches with the real test load-displacement curve. Obviously there would be multiple combination that could satisfy this condition, so we reduce them by fitting them with respect to the lcz material condition which is calculated by a approximate law (rice law). The other hypothesis that we made to reduce even more the calculations is that the critical displacement is the maximum displacement that we have in the lcz region just before the crack extends. Even we know this is not the best choice we have to do that to reduce the calculations even more.

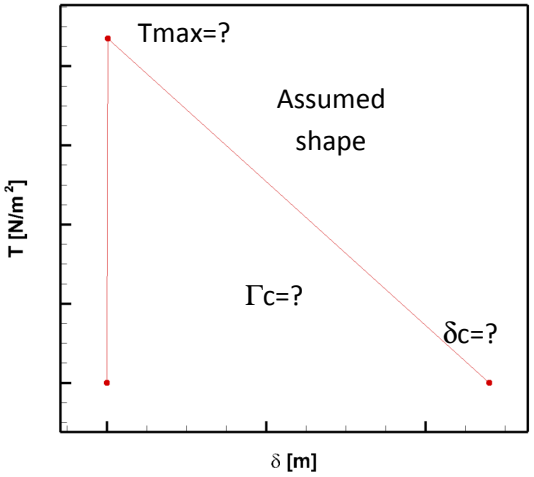

Fig. 5.3.a. A initially rigid triangular law is selected.
There are still three unknowns to be obtained from the test.

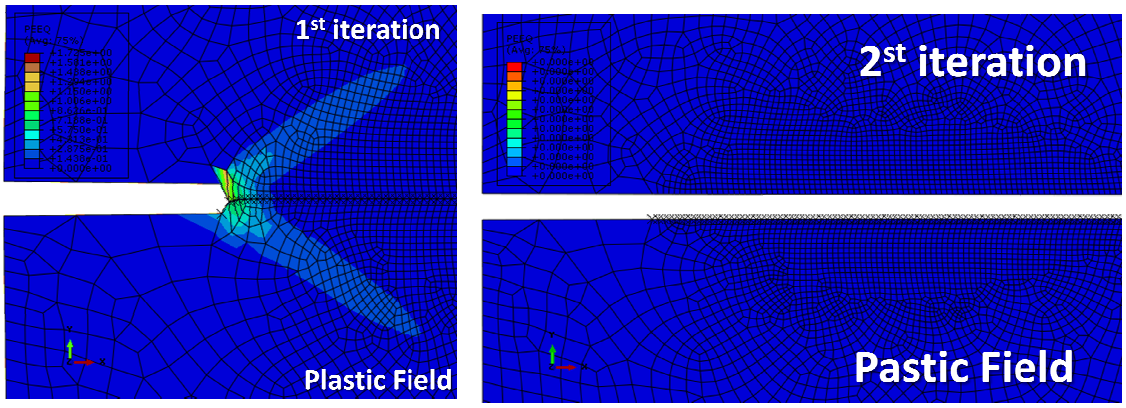

Fig. 5.3.b – Results for the first two iterations. In the first iteration the maximum traction was set as 3 times the yield strength. In the second iteration the maximum traction was reduced one order of magnitude. The element size was defined to be 4 times smaller than the cohesive length (which, interestingly << rp)

Once we set the critical displacement we iterate the maximum traction and energy the required times up to the point we obtain the same Force-displacement curve as the experiments (Fig. 4.f). In our case we run just two iterations in order to study the procedure and check all the assumptions needed to extract this material parameters. In the first iteration the values used where too large and the crack couldn't propagate. In the second run the elements were broken but the result were not good (see fig 5.3.c) and more calculations were needed

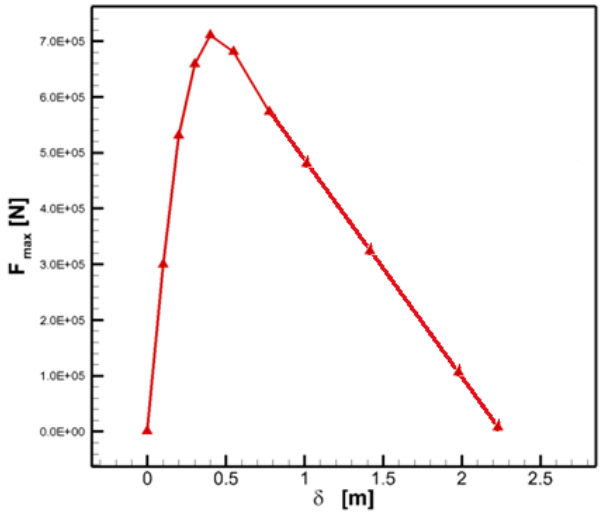

5.3.c Results for second iteration. Notice that the maximum force obtained in the simulation is still around 2.5 times more the peak load in the P-d curve in Fig. 4f.

The conclusions that we obtained from this kind of models is that even they could be used to obtain really detailed parameters of the crack growth, the quantity of hypothesis needed and the precision of the analysis required to make this kind of models requires of experience and a great part of experimental observations. The models required to do reverse-engineering also requires good expertise in numerical calculation and FEM modeling and from an engineering application perspective this kind of material parameters could be difficult to obtain. In addition by observation we assumed that the crack grow in the direction parallel to the crack which could not be true for other loading conditions or specimens. The use of cohesive elements in all the mesh is still an issue in FEM models as the results will result also path dependent in the sense of the element size and distribution.

5.4. - Crack tip Opening Displacement (CTOD).

One of the parameter to characterize the fracture toughness of a metal is the CTOD. We measure this parameter using digital image correlation.

Here we plot the CTOD vs Force

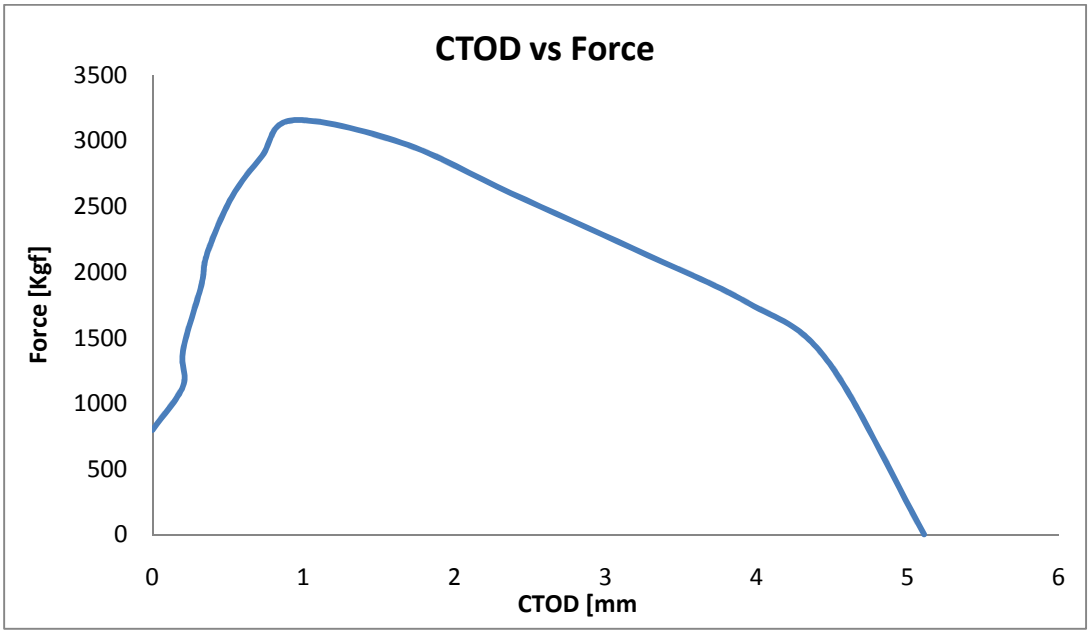

Figure 5.4.a. CTOD vs Force

Also we try to correlate this parameter with the growing distance of the crack Δa. So we plot CTOD vs Δa. We look here for a constant value of Δa with CTOD. But we were not able to notice this in our results due to the width of the sample. We think we need a wither one to notice this behavior. Even though, we showing the plot below

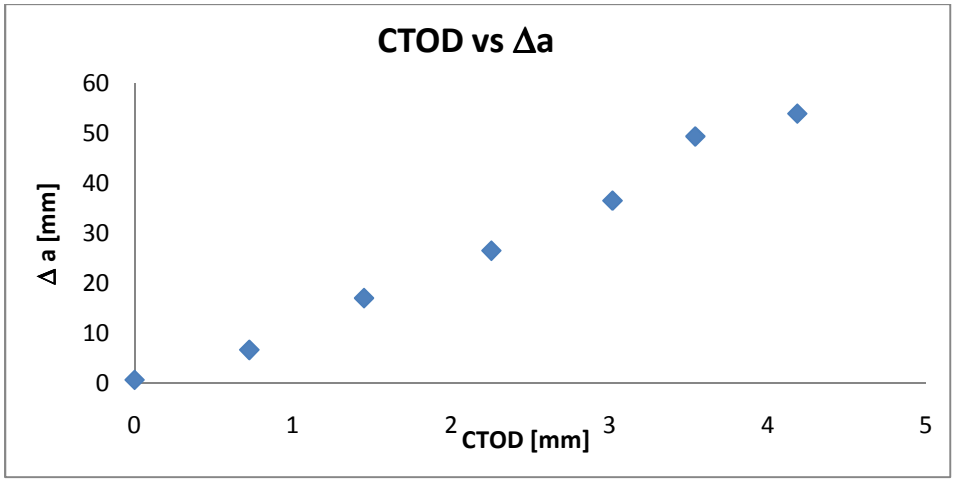

Figure XXXX. CTOD vs Δa.

It was observed by a great quantity of investigators [references] that with the right choice of the size of the specimen size with respect to the crack length constant values of ctod are obtained for a given crack extensions. This supports the concept that the CTOD could be related to a characteristic material parameter to study the crack propagation in materials. If we analyze the curve shown in Fig.5.4.a it can be observed that more than a peak value in the critical load we have a transition closely related to the stable crack growth found in metals. In this sense this kind of curves can be obtained quite easly from the test and used as a comparison with respect to other materials. This method is one of the most used nowadays to characterize fracture in metals and is one of the most cost-effective methods we found.

6.- CONCLUSIONS

- Regardless the design of the sample, our test were in the lower limit of the load cell.
- The displacement device was not adequate in our first tests (Arcan test). Then we change for a more accurate one (lvdt).
- We detect not uniform load displacement in the sample due to slippering between the clamps and the sample.

- We could see a ductile fracture of the aluminum where shear effect dominate the behavior of the fracture shape due to the thickness of the material.
- The arcan fixture works as it was designed. It is a quick tool to test material in mix mode condition. It is easy to implement and attach to any tensile machine.

- The J-integral is not a good parameter for comparison of fracture toughness of a material due to the high presence of plasticity in metal.
- Cohesive models can be used to extract detailed parameters close to the fracture zone but the generation of the cohesive low is difficult and requires assumptions that could lead to mayor errors.
- From a material selection perspective, CTOD criteria would be the best approach to characterize the fracture toughness of a metal.

REFERENCES

[1] Anderson, 2001 “Fracture Mechanics”

[2] Borek, 1998 “Fracture mechanics in engineering practice”

[3] Sutton, et. al. 1999 “Development and application of crack tip opening displacement-based mixed mode fracture criterion”

[4] Cottrell, Pardoen, 2004 “Measuring toughness and cohesive stress-displacement relationship by the essential work of fracture concept”

[5] Greer, et. Al, 2011 “Some comments on the Arcan mixed-mode (I/II) test specimen

[6] Choupani, 2007 “Experimental and numerical investigation of the mixed mode delamination in arcan laminated specimens”

[7] Espinosa, Zavattieri, Dwivedi, 1999 “A 3-D finite deformation anisotropic visco-plasticity model for fiber composites”

[8] Hutchinson, 19xx “Mixed mode fracture mechanics”